Geophysical Research Letters

RESEARCH LETTER
10.1029/2021GL092450

Glaciological Monitoring Using the Sun as a Radio Source for Echo Detection

S. T. Peters[1], D. M. Schroeder[1,2], W. Chu[3], D. Castelletti[2], M. S. Haynes[4], P. Christoffersen[5], and A. Romero-Wolf[4]

[1]Department of Electrical Engineering, Stanford University, Stanford, CA, USA, [2]Department of Geophysics, Stanford University, Stanford, CA, USA, [3]School of Earth & Atmospheric Sciences, Georgia Institute of Technology, Atlanta, GA, USA, [4]NASA Jet Propulsion Laboratory, Pasadena, CA, USA, [5]Scott Polar Research Institute and Department of Geography, University of Cambridge, Cambridge, UK

Key Points:

- We demonstrate a novel "passive" radar sounding approach using the Sun as a radio source to measure ice sheet thickness for the first time
- We evaluate the passive radar's potential to provide continuous records of ice thickness changes, basal conditions, and subsurface processes
- This demonstration charts a course for the development of low-resource, continuous and pervasive monitoring of glacier subsurface conditions

Supporting Information:

Supporting Information may be found in the online version of this article.

Correspondence to:

S. T. Peters,
stpeters@stanford.edu

Citation:

Peters, S. T., Schroeder, D. M., Chu, W., Castelletti, D., Haynes, M. S., Christoffersen, P., & Romero-Wolf, A. (2021). Glaciological monitoring using the Sun as a radio source for echo detection. *Geophysical Research Letters*, *48*, e2021GL092450. https://doi.org/10.1029/2021GL092450

Received 11 JAN 2021
Accepted 28 MAY 2021

Abstract Ice-penetrating radar observations are critical for projecting ice-sheet contribution to sea-level rise; however, these prognostic models have significant uncertainties due to an incomplete understanding of glacial subsurface processes. Existing radars that can characterize subsurface conditions are too resource-intensive to simultaneously monitor ice sheets at both the necessary temporal—daily to multiannual—and spatial—tributary to continental—scales. Here, we investigate using an ambient radio source, instead of transmitting a signal, for glaciological monitoring. We demonstrate, for the first time, passive radio sounding using the Sun to accurately measure ice thickness on Store Glacier, Greenland. Passive radar sounding could provide low-resource time-series measurements of the cryosphere, enabling us to observe and understand evolving englacial and subglacial conditions across Greenland and Antarctica with unprecedented coverage and resolution.

Plain Language Summary Traditional ice-penetrating radars transmit a powerful electromagnetic pulse and record the echo's delay time and power to measure ice sheet thickness and subsurface conditions. While active radar sounding is the principle remote sensing technique used to observe the subsurface of Greenland and Antarctica, existing radar systems are resource-intensive in terms of cost, power, and logistics when simultaneously monitoring ice sheets at both their evolving temporal (daily to multiannual) and spatial (tributary to continental) scales. However, these observations are critical as ice sheet contribution to sea-level rise presents one of the greatest challenges our society faces in the next century. We address this challenge by developing a novel, low-resource, passive radar sounding technique that uses ambient radio signals from the Sun to observe the subsurface of ice sheets at these spatiotemporal scales, instead of transmitting its own powerful radio signal for echo detection. We first demonstrate passive radio sounding using the Sun to accurately measure ice thickness on Store Glacier, Greenland. We then evaluate the passive radar's performance and ability to provide valuable glaciological observations, such as melt rates, bed reflectivity changes, and englacial water storage that have traditionally been obtained using active radar systems but never passively.

1. Introduction

Active radar sounders provide critical measurements of ice sheets (Dowdeswell & Evans, 2004), such as basal melt rates (Khazendar et al., 2016), reflectivity time series (Chu et al., 2016), vertical velocities (Kingslake et al., 2014), ice thickness (Gogineni et al., 2014), englacial water storage (Kendrick et al., 2018), and subglacial conditions (D. A. Young et al., 2016). While active radio sounding is widely used for both airborne and ground-based surveys (Bell et al., 2011; Jenkins et al., 2006), these measurements are expensive and resource intensive when performed for multiple years, with fine temporal resolution, and on spatial scales greater than several kilometers. However, if radar sounders could perform these measurements without transmitting an electromagnetic pulse for echo detection, this would greatly reduce the power consumption, size, design complexity, and cost of the system. Although active systems could also be miniaturized, their low-power transmitted signal would experience geometric power fall-off, whereas a passive sounding technique exploiting a distant source would experience almost no geometric spreading loss and enable lower-resource systems in challenging environments (Schroeder et al., 2016). We have therefore developed

a passive radar that monitors ice sheets by using ambient radio emissions for echo detection (S. T. Peters et al., 2018a, 2018b; Romero-Wolf et al., 2015, 2016; Schroeder et al., 2016).

A potential analog to our developed technique is passive seismic ambient noise correlation, which revolutionized seismological research by using ambient sound waves as a virtual source for measuring properties of the solid Earth (Bensen et al., 2007; Köhler et al., 2015; Ridder et al., 2014). Similar to how passive seismic sensors complement active seismic surveys by using natural and anthropogenic sources instead of exploding dynamite (Bensen et al., 2007; Köhler et al., 2015; Ridder et al., 2014), a receive-only passive radar sounder would use ambient radio waves instead of transmitting a signal for remote sensing (S. T. Peters et al., 2018a, 2018b; Romero-Wolf et al., 2015, 2016; Schroeder et al., 2016). As a low-resource approach, sensor networks of passive sounders could then exploit ambient radio noise to enable cost-effective, multi-year observations of glaciers, ice shelves, and ice sheets with daily resolution at a scale larger than what is currently feasible with active radar systems, but has been accomplished with arrays of passive seismic sensors (Köhler et al., 2015). While other passive radar remote sensing techniques exist (Griffiths & Baker, 2017; Larson et al., 2009), they rely on anthropogenic sources (e.g., GPS and FM radio) that have signal characteristics unsuitable for deep sounding of ice with sufficient resolution. The wide range of potential center frequencies and broad bandwidths provided by radio astronomical sources, such as the Sun (S. T. Peters et al., 2018b) are well suited for radio-echo sounding and yield a device that can monitor frequency-dependent effects of ice sheets with finer range resolution.

Despite these advantages, passive sounding of glaciers using the Sun's ambient radio noise has never been implemented. The passive technique faces three main challenges—all of which we have overcome (S. T. Peters et al., 2018a, 2018b). First, the power level of the Sun in the 200–400 MHz radio frequency band is an order of magnitude below that of the galactic background noise (Figure S13), requiring low noise amplifiers and a sufficient number of samples for the correlation; this is obtained by either increasing the acquisition time (on the order of seconds) or signal bandwidth (on the order of tens of megahertz). Furthermore, anthropogenic radio sources, such as FM stations, TV stations, and electronic equipment, can exceed the Sun's power level; we have addressed this issue by using front-end notch filtering to prevent receiver saturation, and digital signal processing to remove radio frequency interference (RFI) from the acquired signal. Finally, our autocorrelation-based method can be computationally demanding when processing large data volumes; however, on-board correlators could be used to significantly reduce the final stored data volume. We have previously demonstrated the approach's ability to overcoming these challenges posed by the passive system in the Passive Sea Cliff experiment, where our passive prototype used the Sun's radio waves to measure the height of a cliff (S. T. Peters et al., 2018a, 2018b).

Here, we demonstrate passive radio sounding using the Sun as a radio source to measure ice sheet thickness for the first time. In addition to presenting our result from Store Glacier, West Greenland, we evaluate the potential for a passive radar to perform critical observations of subsurface ice sheet processes, such as estimating basal melt rates, glacial bed conditions based on reflectivity changes, and vertical strain rates—all of which have traditionally been performed using active radar systems (Bell et al., 2011; Chu et al., 2016; Dowdeswell & Evans, 2004; Gogineni et al., 2014; Jenkins et al., 2006; Kendrick et al., 2018; Khazendar et al., 2016; Kingslake et al., 2014; D. A. Young et al., 2016). We present passive radio sounding as a novel, low-resource, geophysical technique that has the potential to perform ice-penetrating radar measurements over a much wider range of spatial and temporal scales than active sounding.

2. Materials and Methods

The passive radio sounding technique is the electromagnetic equivalent to passive seismic ambient noise correlation, where ambient sound waves are cross-correlated between seismic stations to invert for terrestrial properties of interest (Bensen et al., 2007; Köhler et al., 2015; Ridder et al., 2014). Similarly, a passive radar receives the Sun's direct and reflected signal, contained in $x(t)$, and an estimate of the signal's autocorrelation can be computed as,

$$C(\tau) = \mathcal{F}^{-1}\left\{\frac{1}{T}\left|X(f,T)\right|_A^2\right\} \quad (1)$$

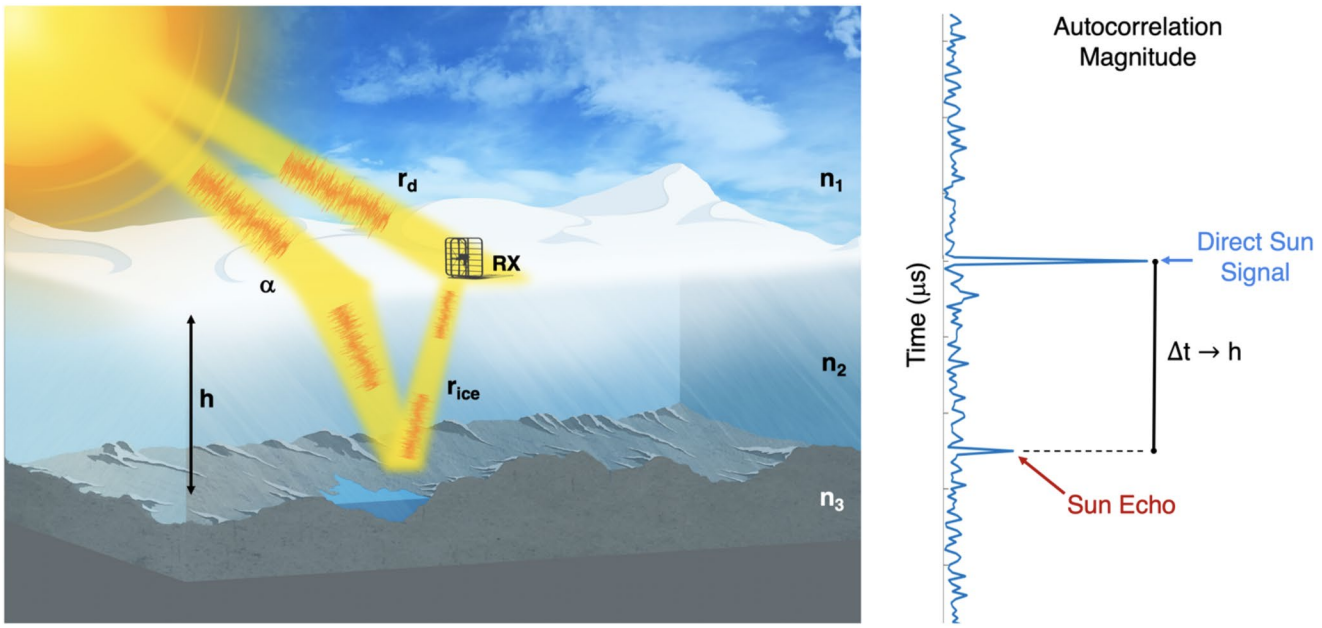

Figure 1. Passive radio sounding concept. (Left) A software-defined radio receiver (RX) sits on the ice sheet's surface and records the Sun's direct path, r_d, and its reflected path, r_{ice}, that is delayed and attenuated as it propagates through the ice. (Right) Treating the received Sun signal as white noise, the autocorrelation-based technique extracts two distinct echo peaks, which correspond to the relative amplitude and delay time between the direct Sun signal and the reflected, attenuated Sun echo (red). The delay time, Δt, between these two peaks in the autocorrelation is then converted to an ice thickness, h, measurement.

where $X(f, T)$ is the T second length Fast Fourier Transform (FFT) of $x(t)$, A denotes amplitude thresholding of the power spectral density (PSD), and $\mathcal{F}^{-1}$ is the inverse FFT. After computing the autocorrelation function, $C(\tau)$, we extract the amplitude and relative delay time of the peaks corresponding to the Sun's direct and reflected paths to measure the glacier's ice thickness (Figure 1).

Converting the echo delay time to a useful ice thickness measurement requires knowledge of the acquisition geometry of the passive sounder, most notably the Sun's elevation angle, α, and azimuth position. Fortunately, this data is easily accessible as the Sun's position is a function of latitude, longitude, date, and time. We assume that the Sun can be treated as an astronomical white noise signal in the radio frequency regime (S. T. Peters et al., 2018b) and that, since the Sun is a distant source, its radio waves arrive as plane waves with constant phase along each wavefront that impinges on the ice sheet (Hecht, 2001).

Exploiting the Sun's spatial coherence and elevation angle allows us to map the echo delay time (Figure 1). As the direct wave travels through the air and the reflected wave travels through the ice sheet, we first divide the path lengths of the Sun's direct ray, r_d, and reflected ray, r_{ice}, by their respective propagation velocities. We then obtain the subsurface angle of incidence, θ_2, from Snell's law, where $n_1 = 1$ is the refractive index of air, and $n_2 = 1.78$ is the refractive index of the ice. From the ice sheet geometry and the Sun's elevation angle, the horizontal distance along the surface between the parallel rays of interests is $x_s = 2h\tan(\theta_2)$. This gives the direct path as $r_d = 2h\tan(\theta_2)\cos(\alpha)$ and the path that propagates through the ice as $r_{ice} = \dfrac{2h}{\cos(\theta_2)}$. The delay time, Δt, between the direct and reflected path is thus:

$$\Delta t = \frac{r_{ice}}{\frac{c}{n_2}} - \frac{r_d}{c} = \frac{2\,h}{\cos(\theta_2)\left(\frac{c}{n_2}\right)} - \frac{2h\tan(\theta_2)\cos(\alpha)}{c} \tag{2}$$

which maps to an ice sheet thickness measurement:

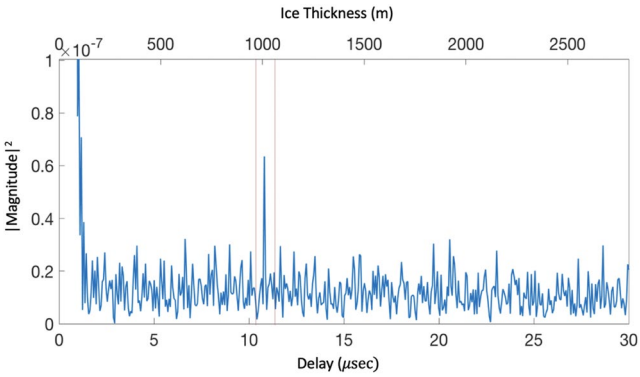

Figure 2. Passive radio sounding measurement taken at Store Glacier, Greenland after filtering radio frequency interference and coherently averaging three consecutive 8-s acquisitions. The distinct echo peak in the autocorrelation function is within the expected delay time for an ice sheet of approximately 1,008 m in thickness. The red vertical lines correspond to the range of expected delay times at the reflection point depth due to any uncertainties in the Sun's elevation, azimuth, and ice sheet geometry as described in Equation 3.

$$h = \frac{\frac{c \cdot \Delta t}{2} cos(\theta_2)}{n_2 - (\sin(\theta_2)\cos(\alpha))} \quad (3)$$

In the limit where $n_2 = n_1 = 1$ and $\theta_2 = \theta_1$, Equation 3 reduces to the same formula as that of the echo delay time in the Passive Sea Cliff experiment, $\Delta t = 2hsin(\alpha) / c \rightarrow h = \frac{c\Delta t}{2sin(\alpha)}$, where the Sun's direct ray and reflected ray off the ocean were measured from the side of a cliff with the same autocorrelation-based technique (S. T. Peters et al., 2018a, 2018b).

2.1. Hardware Configuration

To record the Sun's direct and reflected paths and digitize this signal, we use an Ettus E312 USRP Software-defined radio (SDR). We operate the SDR in receiving mode at a center frequency of 330 MHz with a 15.36 MHz bandwidth. The external frontend of the receiver chain consists of a broadband VHF/UHF skeleton slot antenna and two low noise amplifiers that provide 20 dB of gain each with a 0.5 dB noise figure over a 20 MHz bandwidth. We set the internal gain of the SDR to 62 dB, which gives the SDR its lowest noise figure while minimizing the amount of signal distortion and nonlinearities in the device. We then record each measurement for 8 s, which is the maximum receiving time for our SDR with a 15.36 MHz bandwidth. An extended description of the experiment and selected system parameters is included in the Supporting Information, Text S2.

2.2. Signal Processing Flow

After digitizing the Sun's signal, we then compute its autocorrelation as in Equation 1. We first estimate the PSD of the received data by taking the FFT of the digitized signal and multiplying it by its complex conjugate. We remove any anthropogenic RFI from the signal by amplitude thresholding in the frequency domain, which is a standard method from radio astronomy (Fridman & Baan, 2001), where any signal above the 95th percentile of the PSD is thresholded to the PSD's expected value (S. T. Peters et al., 2018b). We then take the Inverse FFT of the thresholded PSD to obtain the autocorrelation result via the Wiener-Khinchin theorem.

3. Results

We performed our passive radio sounding experiment on Store Glacier, West Greenland (Figure S7). The results of coherently averaging three consecutive passive measurements (Figure S14) after filtering radio frequency interference (Figure S15) show a clear peak in the autocorrelation function at an echo delay time of 10.81 microseconds (Figure 2), which maps to an ice thickness of approximately 1,008 m. We compare the passive radar derived thickness to existing active, ground-based phase-sensitive ApRES radar measurements obtained near our test site and to NASA's Operation IceBridge's Bed Machine v3 ice thickness model (Morlighem et al., 2017) (Figure 3). Our passive measurements agree well with both Bed Machine v3 and ApRES thickness measurements that indicate an ice thickness between 944 and 1,017 m.

To further validate our measurement, we verified that there was no clipping in the received signal's time domain (Figure S1) and that its spectrograms were free of transient RFI (Figure S3). We also estimated the reflection, transmission, attenuation, and scattering losses (M. E. Peters, 2005) (Figure S11) to compare with the anticipated received echo power. After normalizing the autocorrelation, the magnitude of the echo peak is 36 dB below the autocorrelation's zero-delay main lobe, which is comparable to the expected total loss of 35–40 dB at that time (Figure S11). Treating the empirical signal-to-noise ratio (SNR) of the measurement

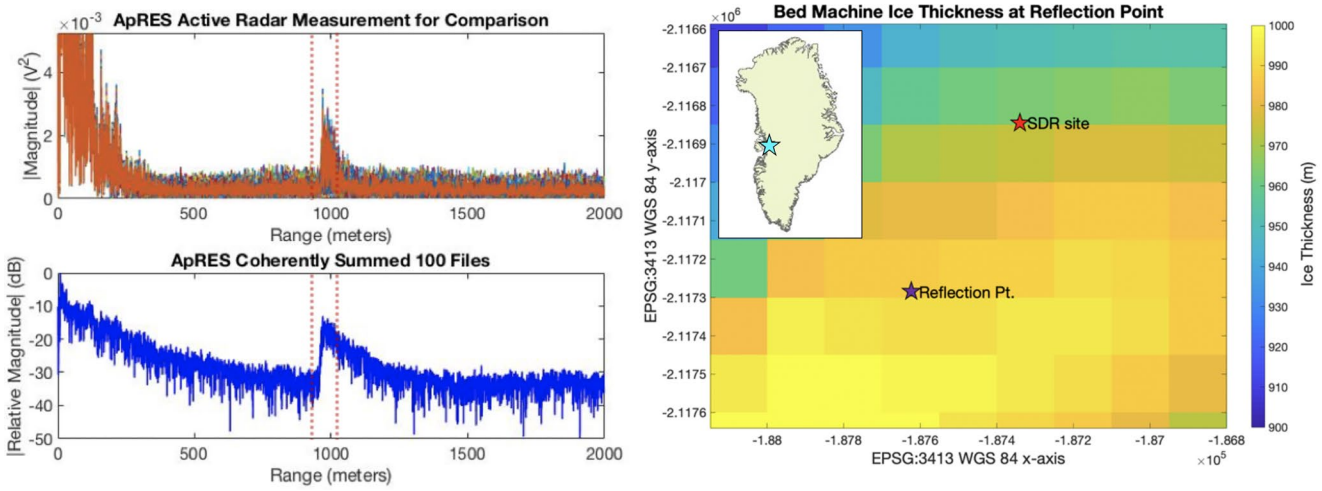

Figure 3. Ground truth validation of passive technique on Store Glacier, Greenland. (Left) Ice thickness measurements ranging from 944 to 1,017 m (red dotted vertical lines) using a ground-based phase-sensitive radar within ±400 m of the Sun's projected reflection point. To increase the signal-to-noise ratio (SNR) of the phase-sensitive radar measurement, we summed 100 chirps (bottom subplot); as such, the falling edge in the active phase-sensitive radar results looks different from the passive measurement due to the white noise's distinct echo peak characteristics and the passive radar's low SNR. We also use the BedMachine v3 model (Right), which agrees with our measured ice thickness, by computing the distance of the Sun's reflection point from its elevation and azimuth angles at the time of acquisition (14:50 local Greenland time). We marked the locations of the software-defined radio position (red star) and Sun's basal reflection point (purple star) at the time of measurement in EPSG:3413 WGS 84 coordinates. The light blue star on the inset map corresponds to Store Glacier (70.56°N, 50.05°W).

as the ratio of the echo peak power to the root-mean-square of the autocorrelation function's noise trail, this echo peak's SNR is 6.4 dB.

The delay time and echo strength obtained with the passive sounder demonstrates its ability to detect a signal that contains the same geometric and radiometric information that one could record using an active sounder at this location. While not demonstrated in this study, our results suggest that dedicated passive radio sounding deployments using the Sun could provide long-term and continuous measurements of ice sheet and ice shelf processes. These include variations in ice thickness, basal melting and refreezing, changes in ice density associated with marine-ice formation, as well as englacial water storage. To project the performance of future passive radar sounding deployments, we provide modeled SNR maps of Greenland and Antarctica (Figure 4). The SNR maps are generated using an ice sheet attenuation and reflectivity model that considers the Sun angle geometry and assumes a thawed bed with a specular subsurface reflection (Supporting Information, Text S4). For each pixel location in the map, the SNR is calculated using the maximum possible integration time for a passive radar receiving at a 330 MHz center frequency with a 15.36 MHz bandwidth. An extended description of the models, parameters, and Sun angle geometry used to generate the SNR maps, as well as more pessimistic cases (e.g., frozen bed, rougher subsurface conditions), is included in the Supporting Information, Text S4 (Figures S16 and S17).

The maximum SNR for passive radar sounding of Greenland and Antarctica is shown for two times of the year—the summer solstice and the spring equinox. The winter solstice SNR map is shown only for Greenland (top, far right), as the majority of Antarctica does not receive sunlight in the winter. Regions with SNR greater than 6 dB represent areas where the passive sounder provides measurements with approximately 90% probability of detection (S. T. Peters et al., 2019). These regions include the major ice shelves of West and East Antarctica, as well as coastal Greenland and the northern and southeastern interior sectors of Greenland. Antarctic ice shelves generally have noticeably high SNR exceeding 60 dB due to their specular subsurface water reflection. In these floating regions, satellite radar (Griggs & Bamber, 2011; Mcmillan et al., 2014; Paolo et al., 2015; Shepherd et al., 2018) and laser altimetry (Brunt et al., 2010; Fricker & Padman, 2006; Pritchard et al., 2012) reveal rapid thinning and ice volume losses due to oceanic warming (Cook et al., 2016; Jenkins et al., 2018; Pritchard et al., 2012; Rignot et al., 2019) and changes in atmospheric conditions (Broeke, 2005; Holland et al., 2019; Scambos et al., 2003; Vaughan et al., 2003). Complementary to these remote sensing observations (Adusumilli et al., 2018; Paolo et al., 2015; Pritchard et al., 2012) passive

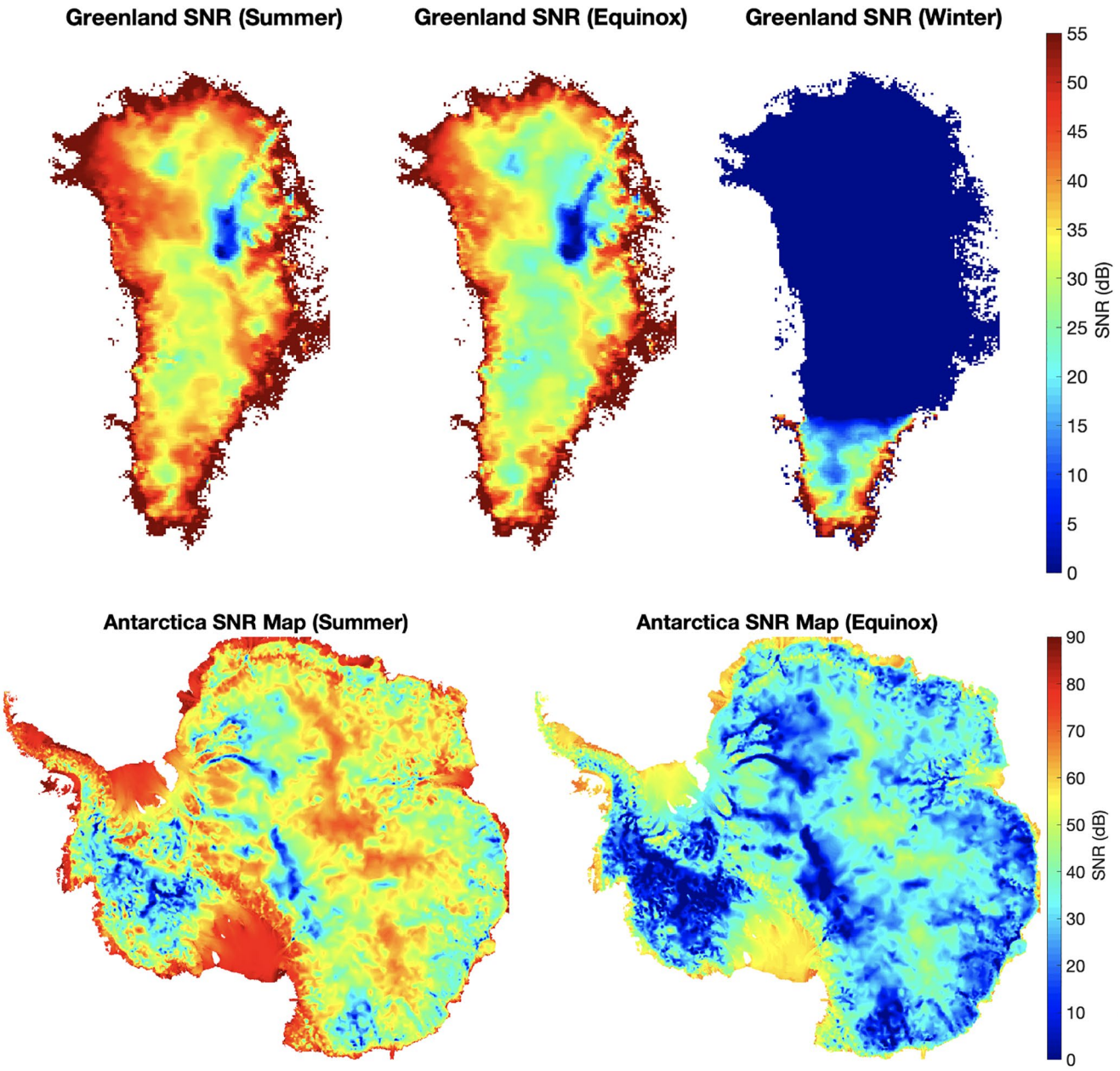

Figure 4. Modeled passive signal-to-noise ratio (SNR) maps of Greenland and Antarctica shown for two times of year—the summer solstice (left) and spring equinox (right). The winter solstice SNR map is shown only for Greenland (top, far right) due to Sun availability. The expected SNR is based on an ice sheet attenuation model, reflection and scattering losses for thawed bedrock, and the maximum integration time with our system's bandwidth. Ice shelves, with a specular reflection from water at the base, are high SNR regions that are ideal targets for passive sounding. Regions with high attenuation and thick ice are challenging targets for a passive radio sounder, as the SNR in these regions is less than 6 dB, even for the maximum integration time. In general, a passive radio sounder can reliably perform ice thickness measurements and phase-sensitive measurements in regions with SNR greater than 6 and 10 dB, respectively (S. T. Peters et al., 2019).

radar sounding can potentially provide measurements at high temporal and spatial resolutions on variations in ice-shelf thickness and ice/ocean-related processes, such as basal melting and refreezing of marine ice beneath the ice shelves.

In Greenland, the coastal regions with less than 1 km of ice have a relatively high SNR above 60 dB, making them excellent targets for passive radar to provide long-term observations of ice thickness and changes in basal conditions. Similarly, high SNR exceeding 50 dB is also present in the interior of Northwestern

Greenland where englacial ice lenses and slabs are formed (Macferrin et al., 2019) and in the Southeastern sector where dynamic englacial firn aquifers exist (Forster et al., 2013; Koenig et al., 2014; Miège et al., 2016; Miller et al., 2018; Poinar et al., 2017). By setting up permanent, long-term deployment stations, similar to what has been done with the Polar Earth Observing Network, passive radar sounding would provide valuable continuous information about how these englacial hydrologic features evolve on daily to interannual timescales.

Since the time-bandwidth product and the ability to coherently average over multiple measurements effectively determines the SNR of the received integrated signal, it is desirable to listen as long as possible, with the widest bandwidth possible, and record as many files as possible while the Sun's reflection stays within a Fresnel zone. Assuming the same antenna footprint, the spatial coverage of a single passive receiver is comparable to a stationary ApRES; however, the passive radar could use the circling Sun to map an annulus of bed topography with a daily temporal resolution. The size of this ring is dependent on the ice thickness at that location; for an ice thickness of 1,000 m, this annulus ranges from 400 to 600 m in radius (Figure S9). Future deployments could use a phased array to steer the receiving antenna beam pattern and repeat these measurements every 24 h as the Sun returns to that reflection point. These results also highlight how the technique could provide time-series measurements of basal reflectivity to infer temporal changes in ice sheet basal conditions. Provided the deployed system obtains an SNR of at least 15 dB, it would be able to closely monitor the changes in reflective power between a thawed and frozen bed (M. E. Peters, 2005). Finally, the high SNR regions (greater than 50 dB) of Figure 4 highlight areas where passive sounding could monitor englacial water storage, where the amount of water storage is proportional to the required SNR.

Future deployments could also monitor melt rates by observing the change in thickness over time with a resolution that is inversely proportional to the bandwidth. With an inherent range resolution of $r = \frac{c}{(2n \cdot \Delta f)}$, the projected ground-range resolution (Griffiths & Baker, 2017) is $r = \frac{c}{(2n \cdot \Delta f \cdot \sin(\theta_2))}$ where c is the speed of light, n is the refractive index of the ice, Δf is the bandwidth of the system, and θ_2 is the subsurface incidence angle. In the case of our experiment, our system has a 15.36 MHz bandwidth that gives a range resolution of 10–20 m depending on the geometry. For our measurement at 14:50 local Greenland time (Figure 2), this gave a ground-range resolution of roughly 12 m. The wide bandwidths provided by radio astronomical sources, such as the Sun, thus provide a fine vertical resolution that is well suited for radio-echo sounding.

We have previously shown that the phase of the autocorrelation's echo peak changes as a function of range in our measurement (S. T. Peters et al., 2019). Even if the echo peak stays at the same sample delay time in the autocorrelation function, the Sun's movement creates a phase change that is a function of range, $\phi = kr = \frac{2\pi r}{\lambda}$. This produces a finer range resolution, $R_{fine} = \frac{\lambda\phi}{4\pi}$, than the inherent range resolution, $r = \frac{c}{2n\Delta f}$, with an accuracy that is a function of SNR (Brennan et al., 2014); the RMS phase noise is $\Delta\phi_{rms} = \frac{1}{\sqrt{2 \cdot SNR}}$ and the RMS range measurement error is $R_{rms} = \frac{\lambda\Delta\phi_{rms}}{4\pi} = \frac{\lambda}{4\pi\sqrt{2 \cdot SNR}}$. By tracking the phase of the passive radar's autocorrelated signal, this would enable submeter precision of glaciological measurements, such as melt rates, vertical velocities, and vertical strain rates, in the same manner as currently done with the active ApRES radar (Brennan et al., 2014). In addition to providing a finer range precision, tracking the phase of the autocorrelation's echo peak would enable finer azimuth resolution and passive synthetic aperture radar focusing (S. T. Peters et al., 2021).

4. Discussion

This proof-of-concept demonstration using an SDR is the first detection of the Sun's echoes through an ice sheet or glacier. The successful measurement of this echo at Store Glacier charts a course for the development of low-resource radar sounding implementations—in terms of data volume, power consumption, instrument size, and cost—that are suitable for catchment to continental-wide monitoring of the ice sheet subsurface at annual to multi-annual timescales. For example, using our current bandwidth of 15.36 MHz

with the maximum integration time of 14 min would require almost 52 gigabytes of memory to store the raw data; however, field-programmable gate array implementations of our autocorrelation-based technique could perform on-board processing and then store the final result to reduce the data volume by more than six orders of magnitude per measurement. Additionally, the development of application-specific integrated circuit chips could perform passive sounding on the order of milliwatts of power (Moser et al., 2019; Wilson et al., 1991) (compared to up to 6 Watts of power drawn by the SDR) to reduce the power consumption by over an order of magnitude. Passive sounding also offers the flexibility to utilize electrically short antennas (Ellingson, 2005; Romero-Wolf et al., 2016) with wide azimuthal beam patterns to reduce the overall system's size relative to active radars; this has led to interest from the planetary science community (Romero-Wolf et al., 2015, 2016; Schroeder et al., 2016), where data, power, and size constraints are even more extreme. Finally, the per unit production for a receive-only radio chip would be less than an active radar system that must transmit and receive. Once miniaturized, a passive sounder could record a measurement, perform on-board processing, and send the result over an Iridium link at modest data rates to provide real-time monitoring. With these future developments, dedicated deployments of passive radar sounding could offer an autonomous, cost-effective, and, therefore, feasible approach to potentially provide continental-wide constraints of evolving ice sheet subsurface conditions on a multi-annual timescale.

This demonstration thus also serves as the first step toward developing advanced passive imaging instruments, such as an array of passive radio sounders, that could perform beam steering and direction finding to track the Sun's subsurface reflection and use long offsets to provide tomographic measurements of the entire 3D volume of the ice and bed (T. J. Young et al., 2018). Passive sounding using ambient radio signals could explore the spatial continuum of phased array versus interferometric measurements, as well as exploit the full radio spectrum—from very low frequency radio waves (as those used for magnetotellerics) to ultra-high frequency Sun and anthropogenic signals. Furthermore, an ultrawideband passive radar that uses spectral stitching (S. T. Peters et al., 2018a, 2018b) could combine both natural (the Sun and Jovian noise) and narrowband anthropogenic sources to achieve extended periods of observations, greater SNR, finer range resolution, and frequency-dependent measurements. By using a variety of sources emanating from different locations and angles, a passive radio sounder could construct a 3D volume of the subsurface and achieve fine temporal monitoring of subsurface glaciological processes.

5. Conclusion

We have demonstrated passive radio sounding using the Sun as a radio source to measure ice sheet thickness for the first time. Our passive radio sounding demonstration opens up the possibility for a wide range of scientifically valuable observations to be passively measured, such as monitoring basal melt rates, englacial water storage, reflectivity time series, and vertical strain rates. As a complement to conventional active radar sounders, a miniaturized, production-ready version of this technique could perform such measurements with reduced power consumption, design complexity, cost, and size. Again, all that is required to produce this result is a receiver that rests on the surface of the ice, passively records the Sun's ambient radio noise, and correlates this signal to estimate the ice thickness. Similar to how passive seismology has enabled cost-effective, large-scale seismic monitoring, future sensor networks of low-resource passive radio sounders could enable us to continuously monitor the Arctic and Antarctic regions, providing an unprecedentedly detailed spatiotemporal window into the subsurface processes that govern their evolution, stability, and sea-level rise contributions.

Acknowledgments
A portion of this work was carried out by the Jet Propulsion Laboratory, California Institute of Technology, under a contract with the National Aeronautics and Space Administration. Dustin Schroeder and Davide Castelletti were also partially supported by a grant from the NASA Cryospheric Sciences. The authors acknowledge Leonardo Carrer for a technical discussion regarding RFI filters and RESPONDER, an ERC-funded research project.

Data Availability Statement

The data set and code for this research are available in S. T. Peters et al. (2021), https://doi.org/10.17632/b69bb5csnp.1.

References

Adusumilli, S., Fricker, H. A., Siegfried, M. R., Padman, L., Paolo, F. S., & Ligtenberg, S. R. M. (2018). Variable basal melt rates of Antarctic Peninsula ice shelves, 1994-2016. *Geophysical Research Letters*, *45*(9), 4086–4095. https://doi.org/10.1002/2017gl076652

Bell, R. E., Ferraccioli, F., Creyts, T. T., Braaten, D., Corr, H., Das, I., et al. (2011). Widespread persistent thickening of the East Antarctic ice sheet by freezing from the base. *Science*, *331*(6024), 1592–1595. https://doi.org/10.1126/science.1200109

Bensen, G. D., Ritzwoller, M. H., Barmin, M. P., Levshin, A. L., Lin, F., Moschetti, M. P., et al. (2007). Processing seismic ambient noise data to obtain reliable broad-band surface wave dispersion measurements. *Geophysical Journal International*, *169*(3), 1239–1260. https://doi.org/10.1111/j.1365-246x.2007.03374.x

Brennan, P. V., Nicholls, K., Lok, L. B., & Corr, H. (2014). Phase-sensitive fmcw radar system for high-precision Antarctic ice shelf profile monitoring. *IET Radar, Sonar & Navigation*, *8*(7), 776–786. https://doi.org/10.1049/iet-rsn.2013.0053

Broeke, M. V. D. (2005). Strong surface melting preceded collapse of Antarctic Peninsula ice shelf. *Geophysical Research Letters*, *32*(12). https://doi.org/10.1029/2005gl023247

Brunt, K. M., Fricker, H. A., Padman, L., Scambos, T. A., & O'Neel, S. (2010). Mapping the grounding zone of the Ross ice shelf, Antarctica, using ICESat laser altimetry. *Annals of Glaciology*, *51*(55), 71–79. https://doi.org/10.3189/172756410791392790

Chu, W., Schroeder, D. M., Seroussi, H., Creyts, T. T., Palmer, S. J., & Bell, R. E. (2016). Extensive winter subglacial water storage beneath the Greenland ice sheet. *Geophysical Research Letters*, *43*(24), 12484–12492. https://doi.org/10.1002/2016GL071538

Cook, A. J., Holland, P. R., Meredith, M. P., Murray, T., Luckman, A., & Vaughan, D. G. (2016). Ocean forcing of glacier retreat in the western Antarctic peninsula. *Science*, *353*(6296), 283–286. https://doi.org/10.1126/science.aae0017

Dowdeswell, J., & Evans, S. (2004). Investigations of the form and flow of ice sheets and glaciers using radio-echo sounding. *Reports on Progress in Physics*, *67*, 1821–1861. https://doi.org/10.1088/0034-4885/67/10/R03

Ellingson, S. W. (2005). Antennas for the next generation of low-frequency radio telescopes. *IEEE Transactions on Antennas and Propagation*, *53*(8), 2480–2489. https://doi.org/10.1109/tap.2005.852281

Forster, R. R., Box, J. E., Broeke, M. R. V. D., Miège, C., Burgess, E. W., Angelen, J. H. V., et al. (2013). Extensive liquid meltwater storage in firn within the Greenland ice sheet. *Nature Geoscience*, *7*(2), 95–98. https://doi.org/10.1038/ngeo2043

Fricker, H. A., & Padman, L. (2006). Ice shelf grounding zone structure from icesat laser altimetry. *Geophysical Research Letters*, *33*(15). https://doi.org/10.1029/2006gl026907

Fridman, P. A., & Baan, W. A. (2001). RFI mitigation methods in radio astronomy. *Astronomy & Astrophysics*, *378*(1), 327–344. https://doi.org/10.1051/0004-6361:20011166

Gogineni, S., Yan, J.-B., Paden, J., Leuschen, C., Li, J., Rodriguez-Morales, F., et al. (2014). Bed topography of Jakobshavn Isbræ, Greenland, and Byrd Glacier, Antarctica. *Journal of Glaciology*, *60*(223), 813–833. https://doi.org/10.3189/2014JoG14J129

Griffiths, H., & Baker, C. (2017). *An introduction to passive radar* (1st ed.). Artech House.

Griggs, J., & Bamber, J. (2011). Antarctic ice-shelf thickness from satellite radar altimetry. *Journal of Glaciology*, *57*(203), 485–498. https://doi.org/10.3189/002214311796905659

Hecht, E. (2001). *Optics* (4th ed.). Addison-Wesley.

Holland, P. R., Bracegirdle, T. J., Dutrieux, P., Jenkins, A., & Steig, E. J. (2019). West Antarctic ice loss influenced by internal climate variability and anthropogenic forcing. *Nature Geoscience*, *12*(9), 718–724. https://doi.org/10.1038/s41561-019-0420-9

Jenkins, A., Corr, H. F., Nicholls, K. W., Stewart, C. L., & Doake, C. S. (2006). Interactions between ice and ocean observed with phase-sensitive radar near an Antarctic ice-shelf grounding line. *Journal of Glaciology*, *52*(178), 325–346. https://doi.org/10.3189/172756506781828502

Jenkins, A., Shoosmith, D., Dutrieux, P., Jacobs, S., Kim, T. W., Lee, S. H., et al. (2018). West Antarctic ice sheet retreat in the Amundsen Sea driven by decadal oceanic variability. *Nature Geoscience*, *11*(10), 733–738. https://doi.org/10.1038/s41561-018-0207-4

Kendrick, A. K., Schroeder, D. M., Chu, W., Young, T. J., Christoffersen, P., Todd, J., et al. (2018). Surface meltwater impounded by seasonal englacial storage in west Greenland. *Geophysical Research Letters*, *45*(19). https://doi.org/10.1029/2018gl079787

Khazendar, A., Rignot, E., Schroeder, D. M., Seroussi, H., Schodlok, M. P., Scheuchl, B., et al. (2016). Rapid submarine ice melting in the grounding zones of ice shelves in west Antarctica. *Nature Communications*, *7*(1). https://doi.org/10.1038/ncomms13243

Kingslake, J., Hindmarsh, R. C. A., Aalgeirsdóttir, G., Conway, H., Corr, H. F. J., Gillet-Chaulet, F., et al. (2014). Full-depth englacial vertical ice sheet velocities measured using phase-sensitive radar. *Journal of Geophysical Research: Earth Surface*, *119*(12), 2604–2618. https://doi.org/10.1002/2014JF003275

Koenig, L. S., Miège, C., Forster, R. R., & Brucker, L. (2014). Initial in situ measurements of perennial meltwater storage in the Greenland firn aquifer. *Geophysical Research Letters*, *41*(1), 81–85. https://doi.org/10.1002/2013gl058083

Köhler, A., Nuth, C., Schweitzer, J., Weidle, C., & Gibbons, S. J. (2015). Regional passive seismic monitoring reveals dynamic glacier activity on Spitsbergen, Svalbard. *Polar Research*, *34*(1), 26178. https://doi.org/10.3402/polar.v34.26178

Larson, K. M., Gutmann, E. D., Zavorotny, V. U., Braun, J. J., Williams, M. W., & Nievinski, F. G. (2009). Can we measure snow depth with GPS receivers? *Geophysical Research Letters*, *36*(17). https://doi.org/10.1029/2009gl039430

Macferrin, M., Machguth, H., As, D. V., Charalampidis, C., Stevens, C. M., Heilig, A., et al. (2019). Rapid expansion of Greenland's low-permeability ice slabs. *Nature*, *573*(7774), 403–407. https://doi.org/10.1038/s41586-019-1550-3

Mcmillan, M., Shepherd, A., Sundal, A., Briggs, K., Muir, A., Ridout, A., et al. (2014). Increased ice losses from Antarctica detected by CryoSat-2. *Geophysical Research Letters*, *41*(11), 3899–3905. https://doi.org/10.1002/2014gl060111

Miège, C., Forster, R. R., Brucker, L., Koenig, L. S., Solomon, D. K., Paden, J. D., et al. (2016). Spatial extent and temporal variability of Greenland firn aquifers detected by ground and airborne radars. *Journal of Geophysical Research: Earth Surface*, *121*(12), 2381–2398. https://doi.org/10.1002/2016jf003869

Miller, O., Solomon, D. K., Miège, C., Koenig, L., Forster, R., Schmerr, N., et al. (2018). Direct evidence of meltwater flow within a firn aquifer in southeast Greenland. *Geophysical Research Letters*, *45*(1), 207–215. https://doi.org/10.1002/2017gl075707

Morlighem, M., Williams, C. N., Rignot, E., An, L., Arndt, J. E., Bamber, J. L., et al. (2017). Bedmachine v3: Complete bed topography and ocean bathymetry mapping of Greenland from multibeam echo sounding combined with mass conservation. *Geophysical Research Letters*, *44*(21). https://doi.org/10.1002/2017gl074954

Moser, D., Tresoldi, G., Schüpbach, C., & Lenders, V. (2019). *Design and evaluation of a low-cost passive radar receiver based on iot hardware* (pp. 1–6). 2019 IEEE Radar Conference (RADARCONF).

Paolo, F. S., Fricker, H. A., & Padman, L. (2015). Volume loss from Antarctic ice shelves is accelerating. *Science*, *348*(6232), 327–331. https://doi.org/10.1126/science.aaa0940

Peters, M. E. (2005). Analysis techniques for coherent airborne radar sounding: Application to west Antarctic ice streams. *Journal of Geophysical Research*, *110*(B6). https://doi.org/10.1029/2004jb003222

Peters, S. T., Schroeder, D. M., Castelletti, D., Haynes, M., & Romero-Wolf, A. (2018a). *First in-situ demonstration of passive radio sounding using the Sun as a source for echo detection* (pp. 4154–4157). International Geoscience and Remote Sensing Symposium (IGARSS), IEEE. https://doi.org/10.1109/IGARSS.2018.8517970

Peters, S. T., Schroeder, D. M., Castelletti, D., Haynes, M., & Romero-Wolf, A. (2018b). In situ demonstration of a passive radio sounding approach using the sun for echo detection. *IEEE Transactions on Geoscience and Remote Sensing*, *56*(12), 7338–7349. https://doi.org/10.1109/TGRS.2018.2850662

Peters, S. T., Schroeder, D. M., Castelletti, D., Haynes, M., & Romero-Wolf, A. (2019). *Two dimensional image formation with passive radar using the sun for echo detection* (pp. 10091–10094). IGARSS 2019—2019 IEEE International Geoscience and Remote Sensing Symposium. https://doi.org/10.1109/IGARSS.2019.8897880

Peters, S. T., Schroeder, D. M., Haynes, M. S., Castelletti, D., & Romero-Wolf, A. (2021). Passive synthetic aperture radar imaging using radio-astronomical sources. *IEEE Transactions on Geoscience and Remote Sensing*, 1–16. https://doi.org/10.1109/TGRS.2021.3050429

Poinar, K., Joughin, I., Lilien, D., Brucker, L., Kehrl, L., & Nowicki, S. (2017). Drainage of southeast Greenland firn aquifer water through crevasses to the bed. *Frontiers in Earth Science*, *5*. https://doi.org/10.3389/feart.2017.00005

Pritchard, H. D., Ligtenberg, S. R. M., Fricker, H. A., Vaughan, D. G., Broeke, M. R. V. D., & Padman, L. (2012). Antarctic ice-sheet loss driven by basal melting of ice shelves. *Nature*, *484*(7395), 502–505. https://doi.org/10.1038/nature10968

Ridder, S. A. L. D., Biondi, B. L., & Clapp, R. G. (2014). Time-lapse seismic noise correlation tomography at Valhall. *Geophysical Research Letters*, *41*(17), 6116–6122. https://doi.org/10.1002/2014gl061156

Rignot, E., Mouginot, J., Scheuchl, B., Broeke, M. V. D., Wessem, M. J. V., & Morlighem, M. (2019). Four decades of Antarctic ice sheet mass balance from 1979–2017. *Proceedings of the National Academy of Sciences of the United States of America*, *116*(4), 1095–1103. https://doi.org/10.1073/pnas.1812883116

Romero-Wolf, A., Schroeder, D. M., Ries, P., Bills, B. G., Naudet, C., Scott, B. R., et al. (2016). Prospects of passive radio detection of a subsurface ocean on Europa with a lander. *Planetary and Space Science*, *129*, 118–121. https://doi.org/10.1016/j.pss.2016.06.010

Romero-Wolf, A., Vance, S., Maiwald, F., Heggy, E., Ries, P., & Liewer, K. (2015). A passive probe for subsurface oceans and liquid water in Jupiter's icy moons. *Icarus*, *248*, 463–477. https://doi.org/10.1016/j.icarus.2014.10.043

Scambos, T., Hulbe, C., & Fahnestock, M. (2003). Climate-induced ice shelf disintegration in the Antarctic Peninsula. In E. Domack, A. Levente, A. Burnet, R. Bindschadler, P. Convey, & M. Kirby (Eds.), Antarctic Peninsula climate variability: Historical and paleoenvironmental perspectives (pp. 79–92). American Geophysical Union (AGU). https://doi.org/10.1029/AR079p0079

Schroeder, D. M., Romero-Wolf, A., Carrer, L., Grima, C., Campbell, B. A., Kofman, W., et al. (2016). Assessing the potential for passive radio sounding of Europa and Ganymede with RIME and REASON. *Planetary and Space Science*, *134*, 52–60. https://doi.org/10.1016/j.pss.2016.10.007

Shepherd, A., Ivins, E., Rignot, E., Smith, B., Broeke, Van den, M., Whitehouse, P., et al. (2018). Mass balance of the Antarctic ice sheet from 1992 to 2017. *Nature*, *558*, 219–222. https://doi.org/10.1038/s41586-018-0179-y

Vaughan, D., Marshall, G., Connolley, W., Parkinson, C., Mulvaney, R., Hodgson, D., et al. (2003). Recent rapid regional climate warming on the Antarctic Peninsula. *Climatic Change*, *60*, 243–274. https://doi.org/10.1023/A:1026021217991

Wilson, J. F., Youell, R., Richards, T. H., Luff, G., & Pilaski, R. (1991). A single-chip VHF and UHF receiver for radio paging. *IEEE Journal of Solid-State Circuits*, *26*(12), 1944–1950. https://doi.org/10.1109/4.104188

Young, D. A., Schroeder, D. M., Blankenship, D. D., Kempf, S. D., & Quartini, E. (2016). The distribution of basal water between Antarctic subglacial lakes from radar sounding. *Philosophical Transactions of the Royal Society A: Mathematical, Physical & Engineering Sciences*, *374*(2059), 20140297. https://doi.org/10.1098/rsta.2014.0297

Young, T. J., Schroeder, D. M., Christoffersen, P., Lok, L. B., Nicholls, K. W., Brennan, P. V., et al. (2018). Resolving the internal and basal geometry of ice masses using imaging phase-sensitive radar. *Journal of Glaciology*, *64*(246), 649–660. https://doi.org/10.1017/jog.2018.54

References From the Supporting Information

Aschwanden, A., Bueler, E., Khroulev, C., & Blatter, H. (2012). An enthalpy formulation for glaciers and ice sheets. *Journal of Glaciology*, *58*(209), 441–457. https://doi.org/10.3189/2012jog11j088

Bendat, J. S., & Piersol, A. G. (2010). *Random data: Analysis and measurement procedures* (4th ed.). John Wiley & Sons, Inc.

Comiso, J. C. (2000). Variability and trends in Antarctic surface temperatures from in situ and satellite infrared measurements. *Journal of Climate*, *13*(10), 1674–1696. https://doi.org/10.1175/1520-0442(2000)013%3C1674:VATIAS%3E2.0.CO;210.1175/1520-0442(2000)013<1674:vatias>2.0.co;2

Cuffey, K., & Paterson, W. S. B. (2010). *The physics of glaciers*. Butterworth-Heinemann.

Dwyer, R. (1983). *Detection of non-gaussian signals by frequency domain kurtosis estimation*. ICASSP 83. IEEE International Conference on Acoustics, Speech, and Signal Processing. https://doi.org/10.1109/icassp.1983.1172264

Ettema, J., Broeke, M. R. V. D., Meijgaard, E. V., Berg, W. J. V. D., Bamber, J. L., Box, J. E., & Bales, R. C. (2009). Higher surface mass balance of the Greenland ice sheet revealed by high-resolution climate modeling. *Geophysical Research Letters*, *36*(12). https://doi.org/10.1029/2009gl038110

Fretwell, P., Pritchard, H. D., Vaughan, D. G., Bamber, J. L., Barrand, N. E., Bell, R., et al. (2013). Bedmap2: Improved ice bed, surface and thickness datasets for Antarctica. *The Cryosphere*, *7*(1), 375–393. https://doi.org/10.5194/tc-7-375-2013

Glen, J. W., & Perutz, M. F. (1955). The creep of polycrystalline ice. *Proceedings of the Royal Society of London. Series A. Mathematical and Physical Sciences*, *228*(1175), 519–538. https://doi.org/10.1098/rspa.1955.0066

Joughin, I., Smith, B. E., Howat, I. M., Scambos, T., & Moon, T. (2010). Greenland flow variability from ice-sheet-wide velocity mapping. *Journal of Glaciology*, *56*(197), 415–430. https://doi.org/10.3189/002214310792447734

Larour, E., Seroussi, H., Morlighem, M., & Rignot, E. (2012). Continental scale, high order, high spatial resolution, ice sheet modeling using the ice sheet system model (ISSM). *Journal of Geophysical Research*, *117*(F1). https://doi.org/10.1029/2011jf002140

Macgregor, J. A., Winebrenner, D. P., Conway, H., Matsuoka, K., Mayewski, P. A., & Clow, G. D. (2007). Modeling englacial radar attenuation at siple dome, West Antarctica, using ice chemistry and temperature data. *Journal of Geophysical Research*, *112*(F3). https://doi.org/10.1029/2006jf000717

Martos, Y. M., Jordan, T. A., Catalán, M., Jordan, T. M., Bamber, J. L., & Vaughan, D. G. (2018). Geothermal heat flux reveals the Iceland hotspot track underneath Greenland. *Geophysical Research Letters*, *45*(16), 8214–8222. https://doi.org/10.1029/2018gl078289

Morlighem, M., Rignot, E., Mouginot, J., Seroussi, H., & Larour, E. (2014). Deeply incised submarine glacial valleys beneath the Greenland ice sheet. *Nature Geoscience*, *7*(6), 418–422. https://doi.org/10.1038/ngeo2167

Morlighem, M., Seroussi, H., Larour, E., & Rignot, E. (2013). Inversion of basal friction in Antarctica using exact and incomplete adjoints of a higher-order model. *Journal of Geophysical Research: Earth Surface*, *118*(3), 1746–1753. https://doi.org/10.1002/jgrf.20125

Rignot, E., Mouginot, J., & Scheuchl, B. (2011). Ice flow of the Antarctic ice sheet. *Science*, *333*(6048), 1427–1430. https://doi.org/10.1126/science.1208336

Seroussi, H., Morlighem, M., Rignot, E., Khazendar, A., Larour, E., & Mouginot, J. (2013). Dependence of century-scale projections of the Greenland ice sheet on its thermal regime. *Journal of Glaciology*, *59*(218), 1024–1034. https://doi.org/10.3189/2013jog13j054

Shapiro, N. (2004). Inferring surface heat flux distributions guided by a global seismic model: Particular application to Antarctica. *Earth and Planetary Science Letters*, *223*(1–2), 213–224. https://doi.org/10.1016/j.epsl.2004.04.011